

NASA DEVELOP National Program

California – Ames



Fall 2022

San Diego Water Resources

Monitoring Pollution Plumes due to Storm and Wastewater Runoff in the San Diego Bay and Tijuana River Estuary to Inform Water Quality Management

DEVELOP Technical Report

Final – 11/14/2022

Ethan Gates (Project Lead)

Max VanArnam

Stefanie Dimayuga Mendoza

Jonathan Szeto

Advisors:

Dr. Dan Sousa (San Diego State University)

Dr. Juan Torres-Pérez (NASA Ames Research Center)

Ben Holt (NASA Jet Propulsion Laboratory)

Dr. Christine Lee (NASA Jet Propulsion Laboratory)

Mariam Ayad (University of California, Santa Cruz)

Fellow:

Lisa Tanh (ARC)

1. Abstract

Stormwater and wastewater runoff are a large source of pollutant discharge along the southern California coast and are a major concern to the health of local communities and ecosystems. In partnership with the Tijuana River National Estuarine Research Reserve and the California Department of Environmental Quality, NASA DEVELOP utilized satellite imagery to visualize and analyze the water quality of the Tijuana Estuary and southern California coast after major storm and wastewater events. Using Landsat 8 Operational Land Imager (OLI) and Sentinel-2 Multispectral Instrument (MSI), we estimated the extent and severity of plumes released from the Tijuana River Estuary. We used remotely sensed turbidity to map the extent of plumes, and used remotely sensed turbidity, Chlorophyll-a (chl-a), and colored dissolved organic matter (CDOM) to quantify and visualize stormwater, wastewater, and mixed-plumes from 2013 to 2022. Furthermore, remotely sensed CDOM, turbidity, and chl-a were validated with in-situ data from NOAA and the San Diego Public Utilities in the San Diego coastal area to evaluate the accuracy of water quality data derived from satellite imagery. End products of this project include maps of stormwater, wastewater, and mixed plumes, tables illustrating the average area, CDOM, turbidity, and chl-a of each plume type, and validation graphs between satellite and in-situ data sources. These end products informed the environmental management of the Tijuana River National Estuarine Research Reserve and the public beaches in San Diego.

Key Terms

plume, remote sensing, water quality, CDOM, turbidity, chlorophyll-a, Tijuana River Watershed, San Diego Bay

2. Introduction

2.1 Background Information

The water quality in coastal regions of San Diego has been negatively impacted by anthropogenic pollution. Stormwater and wastewater are both responsible for causing ocean plumes that can be harmful to humans and the ecosystem (Ayad et al., 2020; Ackerman & Weisberg, 2003). The San Diego coastal area is heavily used for recreational water activities, such as surfing, where plume polluted waters expose users to increased levels of bacteria and other pollutants. These water pollutants can cause acute illnesses (Arnold et al., 2017). When certain water quality metrics, such as bacteria or pollutant concentrations in coastal water, exceed health standards, beaches are closed to avoid adverse health effects (San Diego, 2022). Additionally, San Diego County is home to approximately 200 at-risk plant and animal species including many aquatic species that are on the endangered species list (San Diego, n.d.) which are threatened by these plumes.

Following storm events, pollutants including oils, heavy metals, sewage, etc. that have built up in urban areas, are flushed into rivers and waterbodies. Once the polluted rivers reach the ocean, toxic plumes are created that vary in extent and movement through the coast (Holt et al, 2017). Factors such as tide, wind, and currents are the main drivers of plumes (Warrick et al., 2007). Due to the dynamic nature of the pollutants within storm water plumes, they can be difficult to track with conventional methods such as suspended sediments. Colored dissolved organic matter (CDOM) was found to have a high correlation with plume salinity and is a viable parameter that can be used to track the extent of storm water plumes (Warrick et al., 2007).

There are several wastewater treatment plants located in both the US and Mexico that also create plumes in the ocean as well. Due to the different nature of these plumes, they are referred to as wastewater plumes (Ayad et al., 2020). Wastewater plumes are comprised of sewage and are often not localized at the estuary like storm water plumes. Wastewater is usually discharged at ocean outfalls located offshore, but there are some treatment plants that discharge directly onto beaches. Wastewater plumes are highly mobile and tend to travel along the coast across international boundaries. This creates political tension due to differing regulations for treatment plants.

With these concerns in mind, this project set out to use remote sensing to track and evaluate storm water and wastewater plume trends off the coast of San Diego (*Figure 1*). We utilized satellite imagery from 2013 to 2022 to analyze these plumes by using parameters such as CDOM, chlorophyll-a (chl-a), and turbidity.

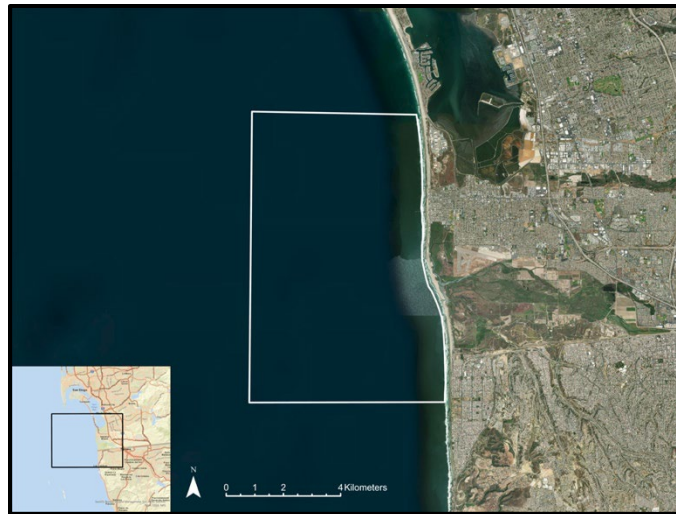


Figure 1. Study area is depicted by a white polygon located along the coast of San Diego, California.

2.2 Project Partners & Objectives

For this project, we partnered with the Tijuana River National Estuarine Research Reserve (TRNERR), San Diego Regional Water Quality Control Board, Waterkeeper Alliance, City of San Diego, and the City of Imperial Beach, and this collaboration sought to better inform partners' stormwater management and water quality improvement efforts. TRNERR is part of the National Estuarine Research Reserve System (NERRS) which is a network of protected areas that were established for long-term research, stewardship, and educational purposes. TRNERR tracks short-term variability and long-term changes in water quality to assist management decisions in protecting the estuary's ecosystem. Waterkeeper Alliance is a nonprofit organization whose efforts lie in preserving and protecting water by connecting and mobilizing more than 300 local Waterkeeper groups around the world. Waterkeeper Alliance addresses critical issues related to clean water and environmental issues. They use position statements to inform their public policy agenda, priorities, advocacy, communications, and all levels of work.

The ultimate aim of this project was to improve the monitoring capabilities of our partners and increase understanding of the runoff extent within San Diego's coastal waters. To do this, we set out to develop maps, charts, and timeseries analyses of coastal water quality. We also aimed to create a Google Earth Engine (GEE) script to delineate plume extent and thus increase ease of pollution monitoring in the study area. By doing so this we enabled partners to determine the effectiveness of treatment plants and best management practices (BMPs) put in place to minimize pollution in the study area.

3. Methodology

3.1 Data Acquisition

3.1.1 Identifying Plume Dates

Precipitation data from NOAA (NCEI, n.d) in conjunction with river flow and wastewater data from the International Boundary and Water Commission (IBWC) were used to identify the dates of stormwater and wastewater plume events (USIBWC, n.d.). The NOAA precipitation data were collected daily at the Brown Field Municipal Airport in San Diego. The IBWC river flow data were collected daily with a flow gage at the international boundary of the Tijuana River approximately six miles from mouth of the estuary. The IBWC wastewater data lists all wastewater spill events that occur at the South Bay International Wastewater Treatment Plant.

3.1.2 Satellite Data

We used the Optical Reef and Coastal Area Assessment (ORCAA) tool (Pippin, H., 2019) to acquire data from Landsat 8 OLI collection 2 level 1 and Sentinel-2 MSI. When collecting satellite data, we sorted for spatial coverage that includes the study area (Figure 1); temporal coverage from March 1st, 2013 to September 30th, 2022; and less than 20% cloud cover.

Table 1. *Satellite Data*

Satellite	Spatial Resolution	Temporal Resolution	Time Period
Landsat 8 OLI	30 m	16 days	Feb 2013 - present
Sentinel-2 MSI	10 m, 20 m	5 days	June 2015 - present

3.1.3 In-Situ Water Quality Data

The CDOM and chl-a *in-situ* measurements were collected by the city of San Diego at various sampling locations off the coast in the San Diego Bay. These samples were collected on a near-daily basis and analyzed in a laboratory onshore. Turbidity *in-situ* measurements were collected by the Boca Rio Water Quality Station within the Tijuana Estuary just east of the mouth of the river. This station collects turbidity measurements in 15-minute intervals and is operated by the NOAA National Estuarine Research Reserve System (NERRS) System-wide Monitoring Program (SWMP). It is important to note that CDOM *in-situ* samples received from the city of San Diego did not have specific timestamps, therefore it was unknown whether they were collected at approximately the time of satellite overpass.

3.2 Data Processing

3.2.1 Identifying Plume Dates

To develop the maps, charts, and time series analyses of coastal water pollution, we identified and classified plumes into stormwater, wastewater, or mixed categories using precipitation data from NOAA and flow data from the IBWC. We sorted the stormwater dates by selecting the top five percent of flow and precipitation dates for all dates with positive values between March 2013 and September 2022. Combined with the dates of all wastewater events, we produced a table of plume dates categorized as stormwater, wastewater or mixed. If the estuary experienced heavy river flow and no wastewater events, then that day is classified as a stormwater plume. If the estuary received only wastewater flow without any rain or flow upstream of the wastewater discharge point, then it is classified as a wastewater plume. If there is any rain or flow in the river on a wastewater event day, then it is classified as a mixed plume. We identified fifteen dates that include five plumes for each of the three types (Table 2).

Table 2.

Plume Dates

Stormwater		Wastewater		Mixed		
Storm Event	Image Capture	Wastewater Event	Image Capture	Storm Event	Wastewater Event	Image Capture
2/27/2022	3/2/2017	2/8/2019	2/8/2019	Continuous	2/23/2017	2/23/2017
12/6/2018	12/7/2018	10/21/2019	10/21/2019	Continuous	3/5/2019	3/5/2019
12/4/2018	12/5/2019	2/13/2020	2/13/2020	1/25/2021	1/28/2021	1/28/2021
12/23/2022	12/27/2019	2/19/2021	2/19/2021	3/3/2021	3/6/2021	3/6/2021
3/3/2022	3/4/2021	2/9/2022	2/9/2022	3/4/2022	3/4/2022	3/4/2022

3.2.2 Calculating CDOM, Turbidity, and Chlorophyll-a with ORCAA

We used the ORCAA 2.0 Google Earth Engine script (Pippin et al., 2019) to process the satellite imagery and output maps of plumes. ORCAA 2.0 uses the GEE simple CloudScore function to mask clouds. Using the algorithm for turbidity (Nechad et al., 2009), the equation for chlorophyll-a (Mishra and Mishra, 2012) and the CDOM equation developed by (Chen et al., 2017), we calculated color dissolved CDOM, turbidity, and chlorophyll-a concentration from satellite surface reflectance data. In ORCAA we produced raster images of these parameters in the study area for each plume date specified in Table 2.

Table 3.

Equations for deriving water quality parameters from Landsat 8 OLI and Sentinel-2 MSI

Calculated Parameter	Equation	Equation #
CDOM	$a_{\text{CDOM}}(440) = 22.283e^{-1.724X}$, $X = \frac{R_{rs}(B3)}{R_{rs}(B5)}$	Equation 1
Turbidity	$\text{Turbidity (FNU)} = \frac{A_T * \rho_w}{1 - \rho_w / C}$	Equation 2
Chlorophyll-a	$[\text{Chlorophyll-a}] = a_0 + (a_1 * \text{NDCI}) + (a_2 * \text{NDCI}^2)$	Equation 3

In finding CDOM, equation 1 only required imagery of Sentinel-2. X is the “remote sensing” or marine reflectance (R_{rs}) of Band B3 (Green) to Band B5 (Red Edge 1).

Turbidity required the use of both Landsat 8 and Sentinel-2 imagery. In Equation 2, A_T , B_T , and C are calibration parameters for which ORCAA uses the respective values of 378.46, 0.33, and 0.19905 for Landsat 8 imagery and 366.14, 0.33, and 0.19563 for Sentinel-2 imagery. Furthermore, ρ_w utilizes the marine reflectance of the 645.5 nm band (Band B4) for both Landsat 8 and Sentinel-2 imagery.

Chlorophyll-a only requires Sentinel-2 imagery to calculate. In equation 3, ORCAA uses 14.039 for a_0 , 86.115 for a_1 , and 194.325 for a_2 . Equation 3 utilizes the Normalized Difference Chlorophyll Index (NDCI). NDCI uses remote sensing reflectance from the 708 nm and 665 nm bands (Bands B5 and B4 respectively) and is described by Mishra and Mishra as:

$$NDCI = \frac{R_{rs}(708) - R_{rs}(665)}{R_{rs}(708) + R_{rs}(665)} \quad \text{Equation 4}$$

3.2.3 Delineating Plume Extent

To map the extent of plumes, we used a threshold value to delineate the area of plume based on turbidity raster images generated by ORCAA in Google Earth Engine (Figure 2a). To find the threshold value, we calculated the 75th percentile/upper quartile of turbidity values in a turbidity raster image of our study area from each stormwater, wastewater, and mixed plume date from Table 2 (Appendix A1). With each individual plume having a turbidity threshold, we took the maximum threshold value within each plume type to use as the threshold for delineating all plumes within that type (Table 4). This resulted in a vector shapefile of plume extent (Figure 2b) for 15 different plumes across three plume types.

Table 4.

Turbidity threshold values from 75th percentile calculation

Plume Type	Turbidity Threshold from 75 th Percentile (FNU)
Stormwater	3.49
Wastewater	1.44
Mixed	1.86

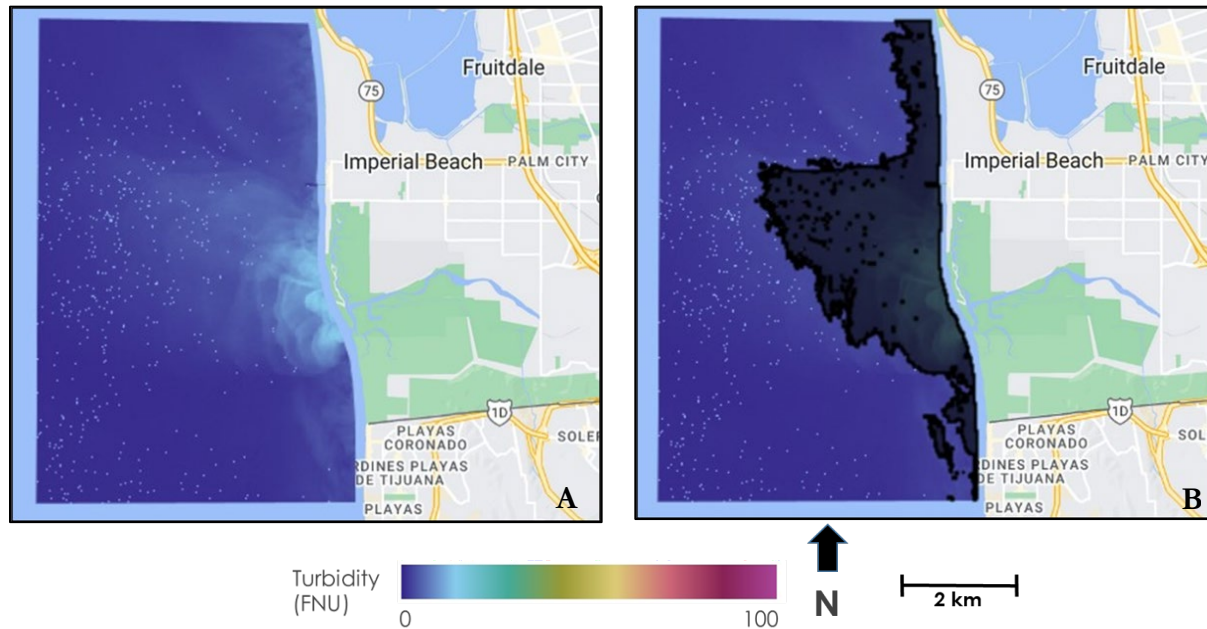


Figure 2. Stormwater turbidity image from Sentinel-2 MSI on 12-5-2019 (left) and plume delineation vector shapefile (right)

3.3 Data Analysis

3.3.1 Calculating Area, Turbidity, Chlorophyll-a and CDOM

Our goal was to study the extent and severity of plumes depending on their source. To compare the extent of plumes, we used GEE to calculate the average area of stormwater, wastewater, and mixed plumes using five plumes for each category. To estimate the severity of each plume type, we used ORCAA to calculate the average CDOM, chlorophyll-a and turbidity for 5 plumes within each plume type (Appendix A1). We then averaged the values for all 5 plumes within each plume type to quantify the severity of stormwater, wastewater, and mixed plumes (Table 5).

3.3.2 Regression Models and Index Validation

To estimate the accuracy of the remotely sensed water quality parameters, we ran a linear regression model between remotely sensed and in-situ CDOM, turbidity, and chlorophyll-a. The results of this analysis quantified the accuracy of the remote sensing analysis performed in this study and illustrated the potential of using satellite imagery to complement in-situ sampling for estimating water quality.

4. Results & Discussion

4.1 Table

The table below shows the average area (km²), CDOM (m⁻¹), chlorophyll-a concentration (mg/m³) and turbidity (FNU) across the five plumes analyzed for each of the three plume types.

Table 5. Area, CDOM, chl-a and turbidity for each plume type

Plume Type	Area (km ²)	CDOM (m ⁻¹)	chl-a (mg/m ³)	Turbidity (FNU)
Stormwater (average)	10.83	1.04	5.59	5.26
Wastewater (average)	8.20	0.12	5.06	1.85
Mixed (average)	10.83	0.34	5.29	2.89

We observe that stormwater and mixed plume areas range from 8-11 km² across the plumes analyzed in this study. Wastewater plumes had the smallest average area of 8.2 km². In comparison of all plume types, CDOM was found to be highest in stormwater plumes by a large margin at 1.04 m⁻¹ in comparison to 0.12 m⁻¹ and 0.34 m⁻¹ in wastewater and mixed plumes, respectively. Chlorophyll-a values were found to be highest in stormwater plumes (5.59 mg/m³) followed by mixed plumes (5.29 mg/m³), and wastewater plumes (5.05 mg/m³). Lastly, turbidity values were found to be the highest for stormwater plumes, followed by mixed plumes with wastewater plumes having the lowest values. The high turbidity values associated with stormwater are likely due to the high sediment load carried by stormwater in the Tijuana River (Ayad et al., 2020).

4.2 Plume Maps

The resulting plume maps are symbolized with each water quality parameter (turbidity, chlorophyll-a and CDOM) for stormwater, wastewater, and mixed type plumes (Figures 3, 4, and 5 respectively).

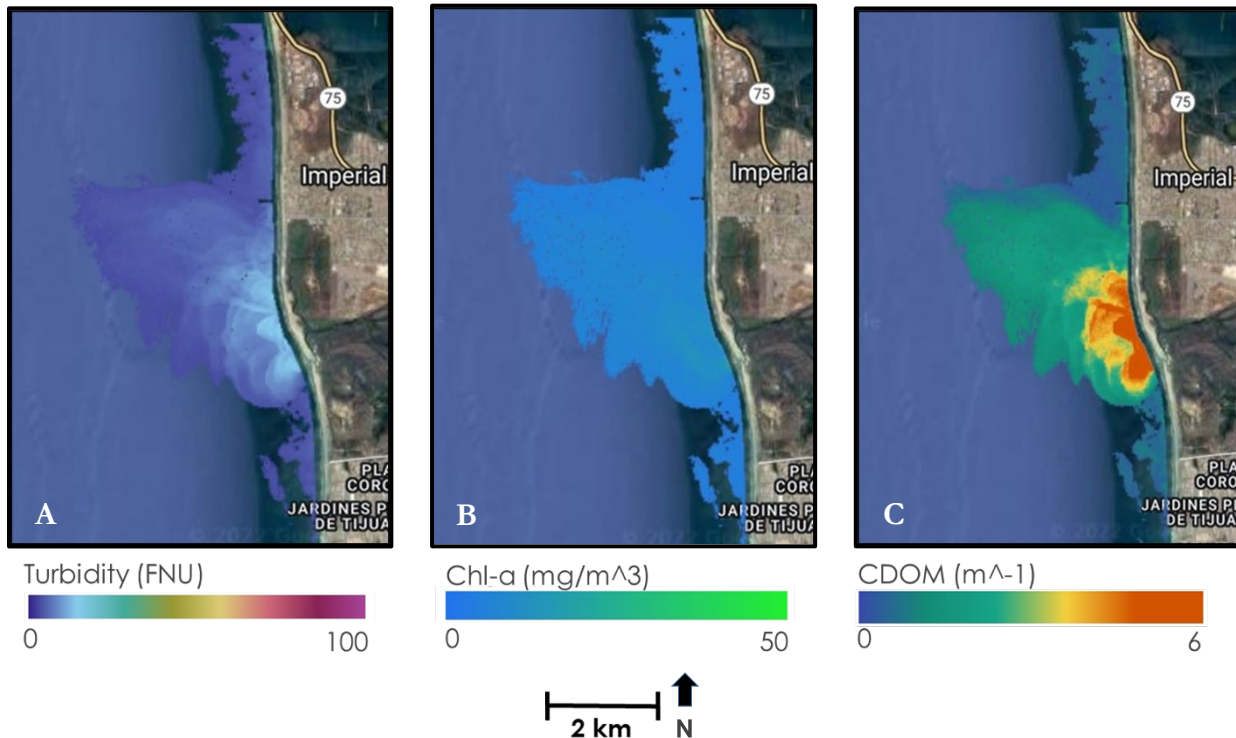


Figure 3. Stormwater turbidity (left), chl-a (center) and CDOM (right) from Sentinel-2 MSI on 12-5-2019

Looking at one of the five stormwater plumes in our study from 12-5-2019 (Figure 3), we see that the average CDOM (1.700 m⁻¹), chl-a (6.836 mg/m³) and turbidity (5.691 FNU) are high when compared to the average values for wastewater and mixed plumes (Appendix A1). These values are also greater than the average

stormwater values of CDOM (1.04 m^{-1}), chl-a (5.59 mg/m^3), and turbidity (5.26 FNU). This data was collected one day after a storm event. We know that the response time for a peak in chlorophyll-a concentration is longer than that of turbidity and CDOM, (Indicators: Chlorophyll a, n.d.) and this could contribute to why we don't see high concentration of chlorophyll-a in this imagery.

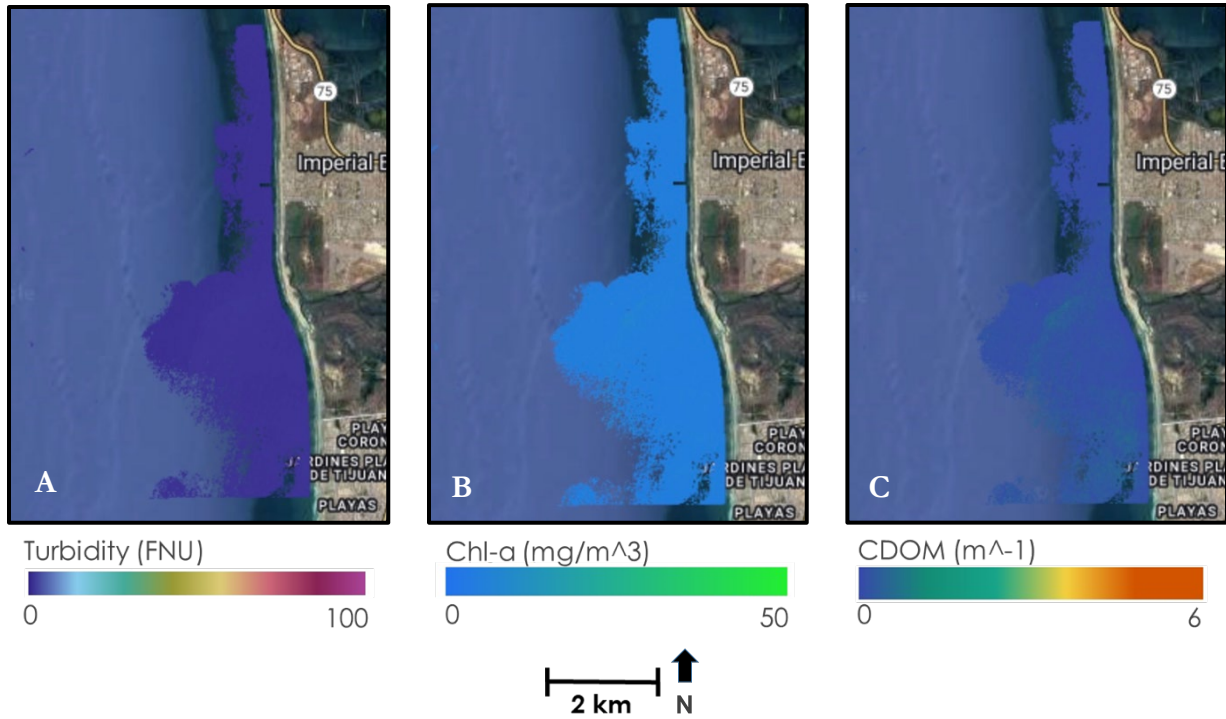
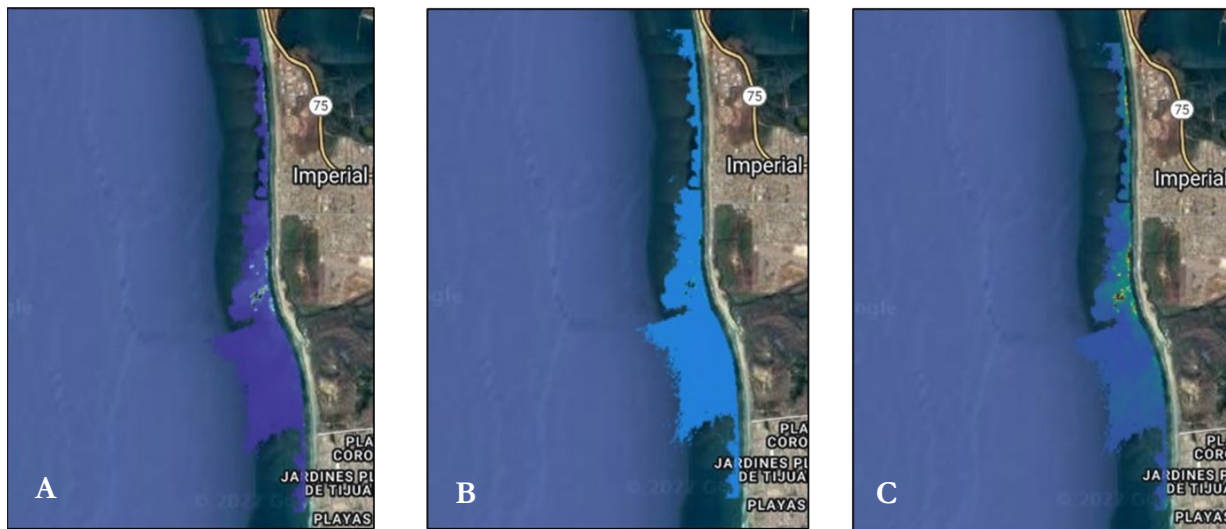


Figure 4. Wastewater turbidity (left), chl-a (center) and CDOM (right) from Sentinel-2 MSI on 2-8-2019

In these water quality maps from less than one day after a wastewater event on 2-8-2019 (Figure 4), we see that average turbidity (1.783 FNU), chlorophyll-a (4.825 mg/m^3), and CDOM (0.046 m^{-1}) are all relatively low when compared to the averages of stormwater and mixed plumes (Appendix A1). This is consistent with the other wastewater plumes analyzed in our study and could be a result of a faster dispersal of pollutants or a discharge too low to be visualized by remote sensing imagery.



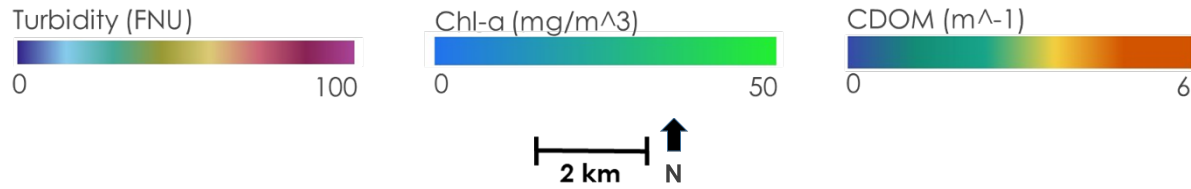


Figure 5. Mixed plume turbidity (left), chl-a (center) and CDOM (right) from Sentinel-2 MSI on 3-6-2021

The mixed plume imagery collected on 3-6-2021 (Figure 5), 3 days after a storm event and one day after a wastewater event, has an average turbidity of (3.206 FNU), average chl-a of (6.146 mg/m³) and average CDOM of (0.517 m⁻¹). These values are higher than the wastewater plumes but lower values than stormwater plumes (Appendix A1). This is consistent with both the other mixed plumes we analyzed and with previous studies on mixed plumes in the region (Ayad et al., 2020).

4.3 Index Validation

CDOM, Turbidity, and chl-a values, derived from Landsat 8 OLI and Sentinel-2 MSI data, were compared to *in-situ* values collected at the various monitoring locations in the San Diego Bay and Tijuana River to evaluate the accuracy of the satellite measurements. Because of the nature in which the three water quality parameters are measured, the sample size of the different indices varied, which also affected the data analysis that was possible. Notably, for the water quality parameters CDOM and chl-a, it was infeasible to evaluate the effectiveness of using satellite imagery to analyze storm, waste, and mixed plumes individually because of the limited number of dates where both *in-situ* data and satellite imagery were available. However, this type of analysis was possible for turbidity since *in-situ* measurements were collected on a near-continuous basis.

Table 6.

Regression model summary statistics for CDOM, chl-a, and Turbidity

Parameter	Equation	R ²	P-values	Sample Size (n)
CDOM (all)	0.804x + 1.64	0.097	5.2E-9	28
chl-a (all)	0.772x + 4.79	0.47	1.93E-7	10
Turbidity (all)	13.2x - 36.1	0.73	0.020	77
Turbidity (Stormwater)	16.0x - 64.4	0.73	0.023	19
Turbidity (Wastewater)	0.0930x + 2.51	0.030	0.32	35
Turbidity (Mixed)	1.56x + 0.517	0.20	0.0025	23

For both CDOM and chl-a, we extracted a 5x5 meter area around the various sampling locations to compute the average value for the respective water quality parameters from the satellite imagery. This average value was then compared with the *in-situ* value sampled on the same date. The CDOM *in-situ* dataset did not contain time values, so it was impossible to verify that CDOM sample collection was done at the same time as satellite overpass. Contrastingly, the chl-a *in-situ* dataset did contain these time values. CDOM has 28 points and chl-a has 10. These points are not differentiated between the various plume types (stormwater, wastewater, or mixed).

The remotely sensed CDOM and chl-a values were found to vary in terms of the correlation between remotely sensed and *in-situ* values ($r^2=0.097$, $n=28$; $r^2=0.47$, $n=10$, respectively). Furthermore, both regression plots were found to be statistically significant as both p-values were less than 0.05, indicating that remote sensing had some capabilities to differentiate between varying levels of *in-situ* concentrations within the study area. Figure 6 is the regression line plots for CDOM and chl-a, respectively.

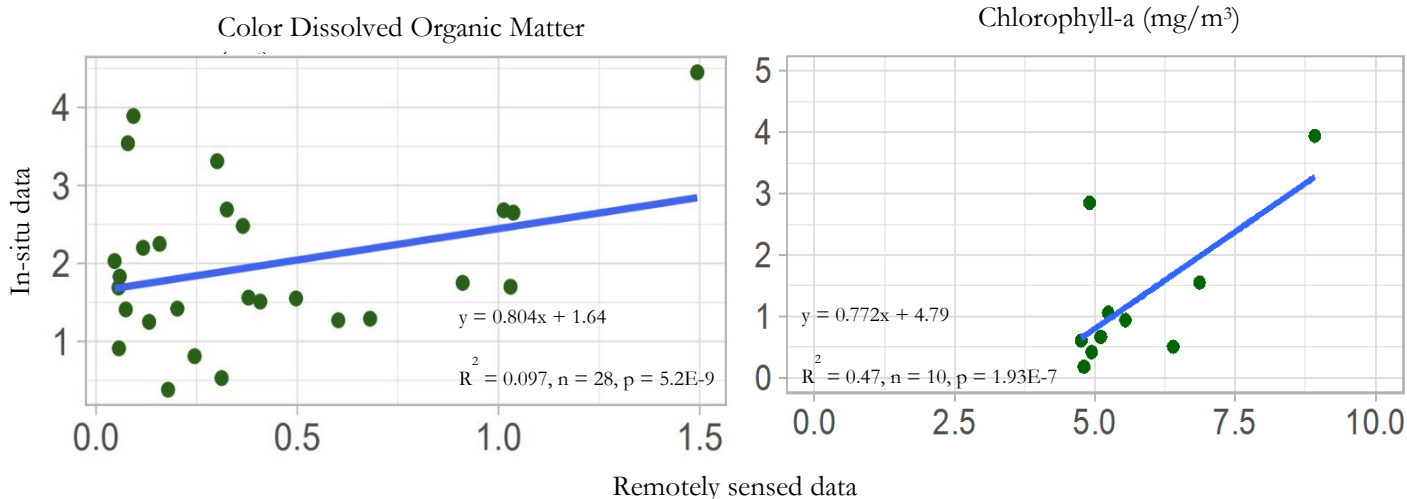


Figure 6. Regression plots for both CDOM and chl-a validation

Overall, in-situ and remotely sensed CDOM did not have high correlation, with the latter tending to underestimate higher in-situ values. However, since there was no way for us to verify that in-situ sampling time overlapped with satellite overpass for our CDOM dataset, our validation for this parameter is less reliable as even within the same day there can be high variation in water quality within the water column in a short time span. Contrastingly, chlorophyll-a *in-situ* and remotely sensed data had a relatively high correlation. However, the small sample size reduces the statistical significance of our model, and more chlorophyll-a samples should be collected on days of satellite overpass to increase the robustness of our regression plot.

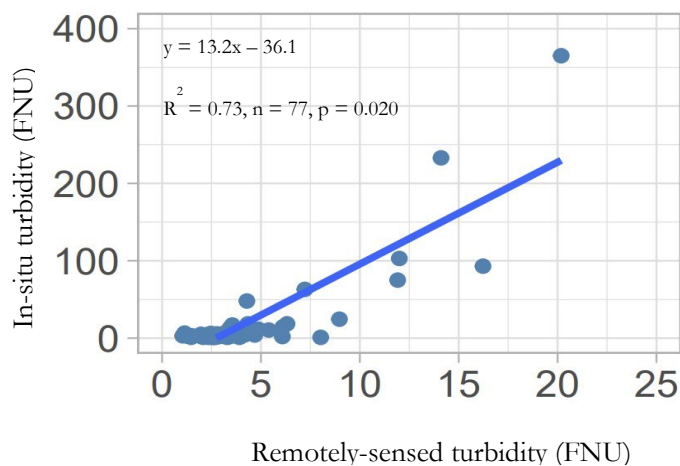


Figure 7. Regression plot for turbidity at the Boca Rio Station. The plot contains 77 points: 19 stormwater, 35 wastewater, and 23 mixed.

For turbidity, we extracted a 5x5 meter area around the Boca Rio Water Quality sampling station to compute

the average turbidity values from the satellite imagery. This average value was then compared with an averaged *in-situ* value sampled on the same date. *In-situ* measurements are collected every 15 minutes, and the measurements at 10:15, 10:30, and 10:45 AM PST (11:15, 11:30 and 11:45 AM PDT) were averaged to account for the slight variability in satellite overpass. Furthermore, we were also able to construct linear regression plots and evaluate remote sensing for measuring turbidity for each event type individually (stormwater, wastewater, and mixed) because more *in-situ* data was available (Figure 8).

The regression plot for turbidity for all events (Figure 7) suggests that remotely sensed values can estimate *in-situ* measurements with relative precision. Turbidity for all events has an R^2 of 0.73 with a sample size of 77. Similarly, p-value of 0.020 indicates a statistically significant relationship between the two variables. However, further analysis on the individual types of plumes in Figure 8 show that remotely sensed data does not measure turbidity well for all plume types. Furthermore, the difference in scale between *in-situ* and remotely sensed turbidity values suggest that remotely sensed data tends to underestimate water quality parameters, especially when these parameters are present at higher magnitudes.

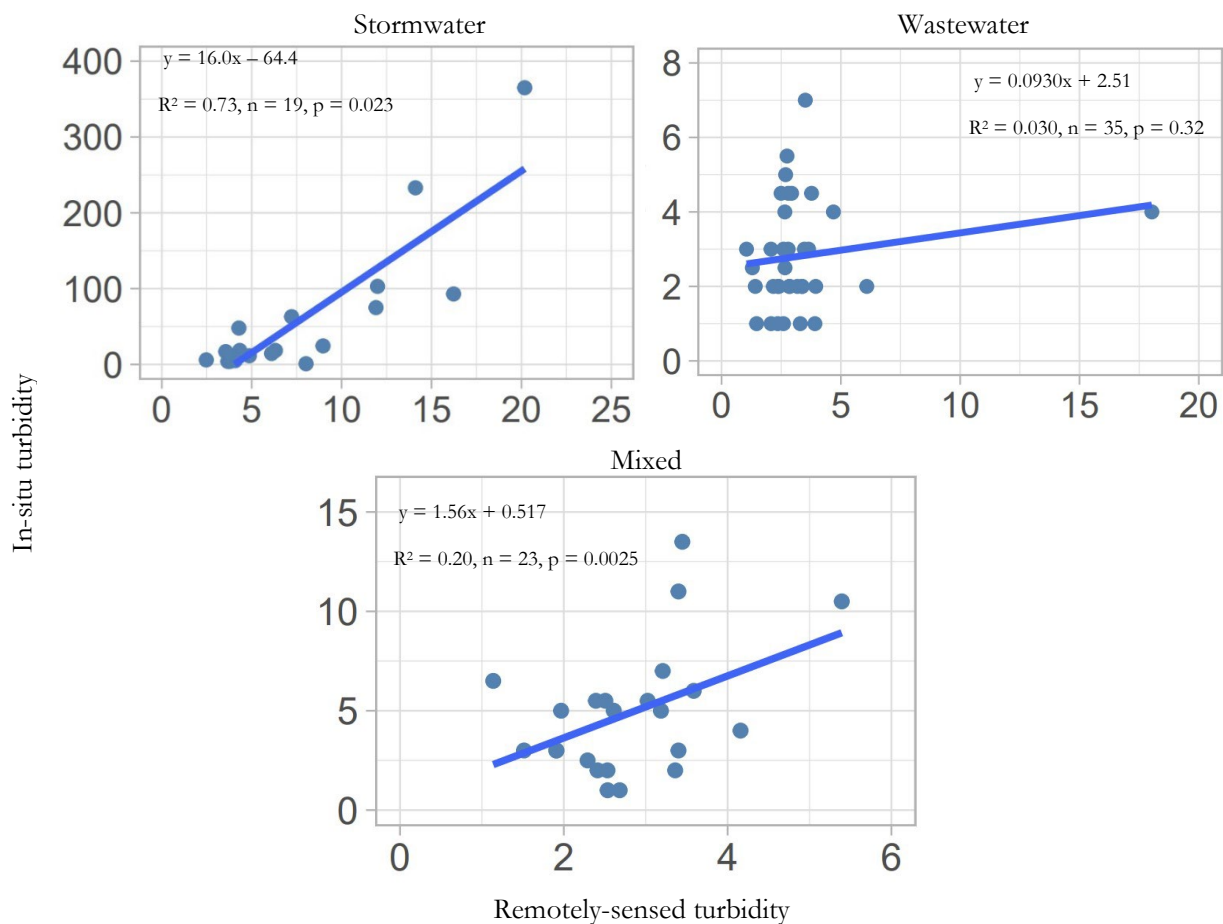


Figure 8. Regression plot for turbidity at the Boca Rio Station for stormwater (top left), wastewater (top right), and mixed (bottom) events. The stormwater plot contains 19 points, wastewater 35, and mixed 23.

The regression plots for each plume classification of stormwater, wastewater, and mixed, illustrate that remote sensing measures turbidity to varying success for each type. The remotely sensed turbidity values correlated strongly with the *in-situ* data provided by our partners for stormwater events, but not wastewater or mixed events ($r^2=0.73$, $n=19$; $r^2=0.03$, $n=35$; $r^2=0.20$, $n=23$ respectively). Thus, stormwater turbidity is not

only the most precisely measured parameter by remote sensing, but it is likely that stormwater turbidity measurements drive the high correlation in the regression plot for turbidity for all events (*Figure 8*). Furthermore, both stormwater and mixed events had a statistically significant relationship between in-situ and remotely sensed data ($p=0.00025$; $p=0.023$, respectively), providing further confidence that remote sensing can be used to estimate turbidity in stormwater and mixed event circumstances. Contrastingly, the high p -value for wastewater events ($p=0.32$) provides evidence that remote sensing cannot adequately measure turbidity within a wastewater context. Stormwater's ability to be more precisely measured by remote sensing comparatively could potentially be explained by the differences in visibility between the different plume types. As seen in Section 4.2 Plume Maps, stormwater plumes are the most visible, which make them easier to analyze by overpassing satellites. Notably, the stormwater regression plot is also the only model that has a large difference in scale between remotely sensed and *in-situ* values. The stormwater plot is the only model with *in-situ* values significantly greater than 10, and the wastewater and mixed plots do not have this same level of discrepancy between *in-situ* and remotely sensed measurements. This provides further evidence that the algorithms used to calculate the three water quality metrics tend to underestimate large values, bringing into the questions of the reliability of remote sensing to measure water quality during high pollution events. This could potentially be caused by a stronger signal-to-noise ratio that is associated with larger pollution events where a higher volume of runoff pollution is involved.

4.4 Errors and Uncertainties

Due to the dynamic nature of ocean plumes, they are difficult to directly compare. Winds and ocean currents have high variability and can have a large impact on plume dispersion. The plumes measured in this study could have been dispersed through oceanic processes that might skew the plume area calculations along with the water quality metrics. Additionally, plumes are not homogeneous in concentration throughout the water column and the remotely sensed measurements only show the surface of the water. Plumes that were subsurface could have been misrepresented by remote sensing techniques.

Turbidity was the water quality metric used to map the extent of the plumes. Due to the proximity to the coast, turbidity caused by wave action likely interfered with the mapping of plume extent. To help prevent this, a buffer along the shoreline was hand drawn so that wave action along the coast could be avoided, although it may have not been large enough to crop out all turbidity caused by wave action. Additionally, this buffer also cut off a section of the plumes which also would interfere with area and water quality metric calculations.

CDOM data was collected daily by the City of San Diego, and we were unable to verify that the *in-situ* measurements were collected at or near the time of satellite overpass in the study area. Since there can be considerable variability in the water column within a day, this reduces the confidence of the CDOM regression plot. The chl-*a* regression plot relied on a low number of observations. Stronger trends might be observed with more observations. In generating the stormwater turbidity regression plot, we found that remotely sensed values can be underestimated when the *in-situ* values become greater than 20 by nearly twentyfold. This could be explained by several reasons. The algorithm used to calculate turbidity from satellite imagery might be biased towards lower values. Additionally, wave action or ocean dynamics at the mouth of the estuary where turbidity values are collected could be skewing the estimates.

4.5 Future Work

Currently, the delineation script we created in Google Earth Engine uses turbidity as the threshold metric to isolate the pollution plumes from its surroundings. While turbidity seemed to be successful at delineating the extent of the plume, there were various instances in which certain parts of the plume did not appear to be encapsulated within the delineation results. Future projects could attempt to evaluate other algorithms for mapping plumes that are less sensitive to wave action or other ocean processes.

Moreover, while we were able to analyze plumes at different stages of development, we were unable to track the spatiotemporal evolution of individual plumes. Using satellite imagery with higher temporal resolution would allow the us to characterize the initiation, maturation, and dispersal of individual plumes. This is not possible with current satellite data alone since Sentinel-2 has a temporal resolution of 5 days. Improvement in spectral resolution would also allow more accurate evaluation of plume severities. Specifically, hyperspectral imagery could provide more accurate and precise estimates of existing plume metrics, as well as enable the development of new metrics. Furthermore, the use of Synthetic Aperture Radar would further increase the image record by allowing data collection regardless of cloud cover which is typically persistent during and after storm events.

There are other water quality metrics that may be analyzed to characterize the severity of plumes in addition to the metrics used in our study. CDOM, chl-a and turbidity were analyzed in this project due to the readily available *in-situ* data and the ubiquity of these metrics in the scientific literature. However, future studies may attempt to analyze other important metrics that are indicative of water quality, such as dissolved oxygen or bacteria concentration.

Future in-situ sampling should be done at satellite overpass time (10:30 AM PST/11:30 AM PDT) to ensure an accurate and reliable regression model. Additionally, future endeavors should include more chl-a measurements on days of satellite overpass to improve the robustness of our model and further validate the remotely sensed water quality indexes.

5. Conclusions

Toxic ocean plumes caused by runoff have threatened costal water quality in San Diego and are both a public health and ecological concern. However, differing plume types can form depending on the source of the coastal runoff with varying extends and severities. We produced a script that enables partners to visualize pollution plumes and quantify their extent and severity. We also produced various maps to compare the extent and severity of the three different plume types, storm, water, and mixed. The differentiation between storm water and wastewater plumes has not been studied extensively until recently (Ayad et al., 2020). Analysis of these maps generated from the tool demonstrated that these different classifications have noticeable visual and chemical distinctions. The results indicate that stormwater and mixed plumes have a much larger extent than wastewater plumes. Similarly, though chl-a concentrations were relatively equivalent amongst all three plume types, stormwater plumes had noticeably higher levels of CDOM and turbidity. Understanding the differences between these plumes will allow the city to make more informed decisions on beach closure polices to protect the health of city citizens. Notably, given the greater extent and severity of stormwater plumes, longer and stricter beach closure polices could be enacted directly after large rain events to ensure public safety. The quantification of wastewater plume extent after runoff events will also allow policy makers to make more informed decisions regarding load standards for new treatment plants and BMPs.

Validation of remotely sensed data with in-situ measurements also evaluates the use of remote-sensing for estimating water quality in our study area. Remote sensing would potentially allow our partners to estimate water severity over a much larger area than possible with in-situ sampling. However, this is only achievable if remote sensing can approximate these indices with accuracy and precision. Our initial validation illustrates that though there is potential for remote sensing to be effective, more work needs to be done to improve the estimation tool. While chl-a and turbidity for stormwater events had strong correlations between remotely sensed and in-situ data, CDOM, and turbidity for all other conditions saw high variation between these measurements. Similarly, turbidity for stormwater events saw a huge difference in scale between in-situ and remotely sensed data, indicating that remote sensing tends to underestimate larger values. Overall, our results show that remote sensing has the precision necessary to potentially be an effective tool for evaluating water quality, but further work needs to be done to make the algorithms that calculate these values more accurate.

6. Acknowledgments

We would like to thank our partners from the Tijuana River National Estuarine Research Reserve (TRNERR), San Diego Regional Water Quality Control Board, City of San Diego, City of Imperial Beach, and Waterkeeper Alliance for their collaboration and input on the project. We also would like to give a special thank you to our science advisors Dr. Juan Torres-Pérez, Dr. Daniel Sousa, Benjamin Holt, Dr. Kenton Ross, Dr. Christine Lee, Mariam Ayad, and also our Node Fellow Lisa Tanh for their continued support throughout this term. Finally, we thank the DEVELOP Project Coordination team Laramie Plott and Cecil Byles for their guidance and editing.

This material contains modified Copernicus Sentinel data (2021), processed by ESA.

Any opinions, findings, and conclusions or recommendations expressed in this material are those of the author(s) and do not necessarily reflect the views of the National Aeronautics and Space Administration.

This material is based upon work supported by NASA through contract NNL16AA05C and 80NSSC22K0907.

7. Glossary

Earth observations – Satellites and sensors that collect information about the Earth’s physical, chemical, and biological systems over space and time

BMP – Best management practice

Colored dissolved organic matter – Water quality parameter that measures the amount of dissolved carbon-based compounds detectable by remote sensing.

Chlorophyll-a – Photosynthetic pigment found in chloroplasts of plants, algae, and plankton

Turbidity – A parameter of water clarity that quantifies that amount of suspended matter

Google Earth Engine – Online platform that combines satellite imagery and geospatial datasets with analytical capabilities.

8. References

- Ackerman, D., & Weisberg, S. B. (2003). Relationship between rainfall and beach bacterial concentrations on Santa Monica Bay beaches. *Journal of Water and Health* 1(2), 85-89. <https://doi.org/10.2166/wh.2003.0010>
- Arnold, B. F., Schiff, K. C., Ercumen, A., Benjamin-Chung, J., Steele, J. A., Griffith, J. F., Steinberg, S. J., Smith, P., McGee, C. D., Wilson, R., Nelsen, C., Weisberg, S. B., & Colford, J. M. (2017). Acute illness among surfers after exposure to seawater in dry- and wet-weather conditions. *American Journal of Epidemiology*, 186(7), 866–875. <https://doi.org/10.1093/aje/kwx019>
- Ayad, M., Li, J., Holt, B., & Lee, C. (2020). Analysis and Classification of Stormwater and Wastewater Runoff From the Tijuana River Using Remote Sensing Imagery. *Front. Environ. Sci.* 8:599030. <https://doi.org/10.3389/fenvs.2020.599030>
- Chen, J., Chu, W., Tian, Y.Q., Yu, Q., Zheng, Y., & Huang, L. (2017). Remote estimation of colored dissolved organic matter and chlorophyll-a in Lake Huron using Sentinel-2 measurements. *Journal of Applied Remote Sensing*, 11(3). <https://doi.org/10.1117/1.JRS.11.036007>
- Copernicus Sentinel-2 MSI Level 1C Data. [2013-2019]. Retrieved from Google Earth Engine, processed by ESA. https://developers.google.com/earth-engine/datasets/catalog/COPERNICUS_S2
- Indicators: Chlorophyll a*. Environmental Protection Agency. (n.d.). Retrieved November 17, 2022. <https://www.epa.gov/national-aquatic-resource-surveys/indicators-chlorophyll>

- Holt, B., Trinh, R., & Gierach, M. M. (2017). Stormwater runoff plumes in the Southern California Bight: A comparison study with SAR and MODIS imagery. *Marine Pollution Bulletin*, 118(1-2), 141–154. <https://doi.org/10.1016/j.marpolbul.2017.02.040>
- Mishra, S., & Mishra, D. R. (2012). Normalized difference chlorophyll index: A novel model for remote estimation of chlorophyll-a concentration in turbid productive waters. *Remote Sensing of Environment*, 117, 394-406. <https://doi.org/10.1016/j.rse.2011.10.016>
- Nechad, B., Ruddick, K. G., & Neukermans, G. (2009). Calibration and validation of a generic multisensor algorithm for mapping of turbidity in coastal waters. In C. R. Bostater Jr., S. P. Mertikas, X. Neyt, & M. Velez-Reyes (Eds.), *SPIE Remote Sensing of the Ocean, Sea Ice, and Large Water Regions 2009* (Proceedings Volume 7473, 74730H). <https://doi.org/10.1117/12.830700>
- National Centers for Environmental Information (NCEI). (n.d.). *Datasets | Climate data online (CDO) | National climatic data center (NCDC)*. <https://www.ncei.noaa.gov/cdo-web/datasets>
- Pippin, H., Valenti, V., Olarte, A., & Pilot, R. (2019). *Belize & Honduras Water Resources II: Developing a Google Earth Engine Dashboard for Assessing Coastal Water Quality in the Belize and Honduras Barrier Reefs to Identify Adequate Waste Control and Inform Coastal Resource Monitoring and Management*. NASA DEVELOP National Program, California – Pasadena. <https://develop.larc.nasa.gov/2019/fall/BelizeHondurasWaterII.html>
- San Diego County Beach Status*. San Diego Coastkeeper. (2022, October 3). Retrieved October 9, 2022. <https://www.sdcoastkeeper.org/beach-advisories>
- San Diego is the most biologically rich county in the continental U.S.* *The Nature Conservancy*. (n.d.). <https://www.nature.org/en-us/get-involved/how-to-help/places-we-protect/san-diego-county/#:~:text=Protecting%20Habitats%20and%20Clean%20Water&text=Endangered%20species%20include%20California%20songbirds,and%20San%20Diego%20fairy%20shrimp>.
- Tijuana River National Estuarine Research Reserve. (2022, May). Monitoring. TRNERR Website. <https://trnerr.org/what-we-do/research/monitoring/>
- US Geological Survey Earth Resources Observation and Science Center. (2014). Landsat 8 OLI/TIRS Level-2 Data Products - Surface Reflectance [Dataset]. <https://doi.org/10.5066/F78S4MZJ>
- USIBWC Water Data Portal*. USIBWC Water Data. (n.d.). Retrieved November 17, 2022, <https://waterdata.ibwc.gov/>
- Warrick, J. A., DiGiacomo, P. M., Weisberg, S. B., Nezlin, N. P., Mengel, M., Jones, B. H., Ohlmann, J. C., Washburn, L., Terrill, E. J., & Farnsworth, K. L. (2007). River plume patterns and dynamics within the Southern California bight. *Continental Shelf Research*, 27(19), 2427–2448. <https://doi.org/10.1016/j.csr.2007.06.015>

9. Appendices

Appendix A.

Table A1

Complete area, CDOM, chl-a and turbidity results

Plume Type	Area (km²)	CDOM (m⁻¹)	Chl-a (mg/m³)	Turbidity (FNU)
Stormwater				
3/2/2017	3.167	0.474	4.839	4.530
12/7/2018	9.091	1.179	5.242	6.216
12/5/2019	15.03	1.700	6.836	5.691
12/27/2019	18.34	0.609	4.865	5.042
3/4/2021	8.515	1.231	6.187	4.843
Average	10.83	1.038	5.594	5.264
Wastewater				
2/8/2019	15.88	0.046	4.825	1.783
10/21/2019	3.194	0.105	4.665	1.798
2/13/2020	2.356	0.118	5.438	1.627
2/19/2021	9.163	0.241	5.663	2.222
2/9/2022	10.40	0.109	4.687	1.806
Average	8.197	0.124	5.056	1.8472
Mixed				
2/23/2017	15.38	0.454	5.050	4.222
3/5/2019	6.960	0.227	5.336	2.169
1/28/2021	5.060	0.155	4.843	2.421
3/6/2021	5.782	0.517	6.146	3.206
3/4/2022	21.00	0.354	5.061	2.417
Average	10.83	0.341	5.287	2.887

Appendix B.

Table B1

Complete turbidity threshold values calculated using the 75th percentile

Event Dates	Turbidity Threshold from 75th Percentile (FNU)
Stormwater	
3/2/2017	2.484
12/7/2018	2.439
12/5/2019	3.406
12/27/2019	3.485
3/4/2021	2.368
Wastewater	
2/8/2019	1.441
10/21/2019	0.953
2/13/2020	1.203
2/19/2021	1.090
2/9/2022	1.328
Mixed	
2/23/2017	1.864
3/5/2019	1.559
1/28/2021	1.356
3/6/2021	1.336
3/4/2022	1.858

Appendix C.

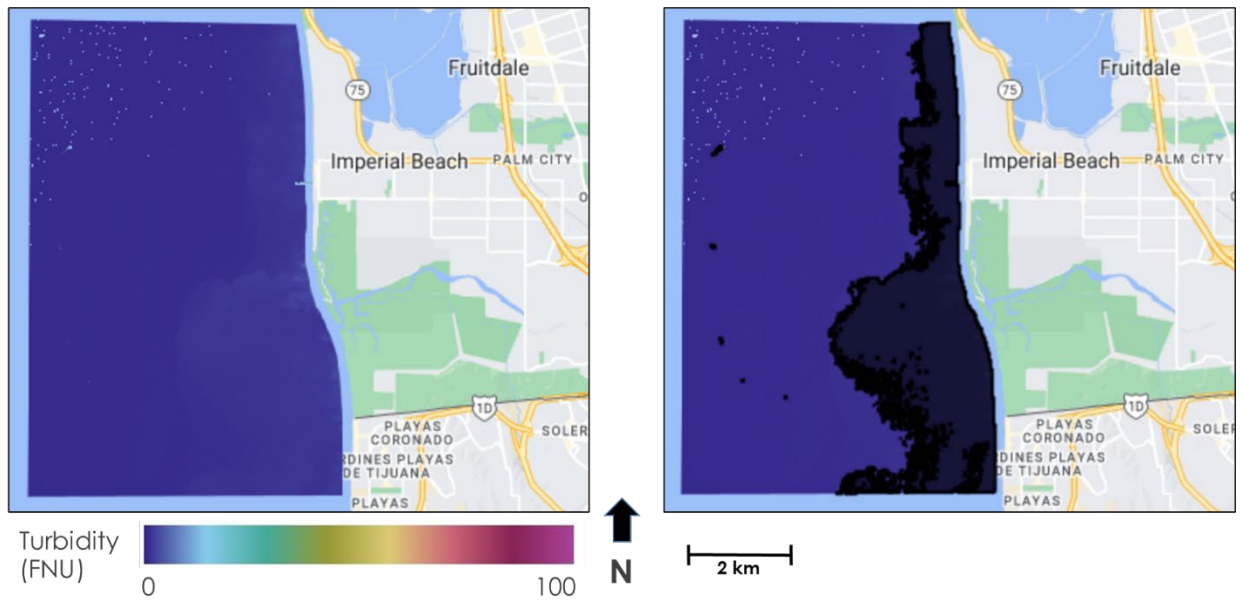


Figure C1. Wastewater plume turbidity image from Sentinel-2 MSI on 2-8-2019 (left) and the plume delineation shapefile (right)

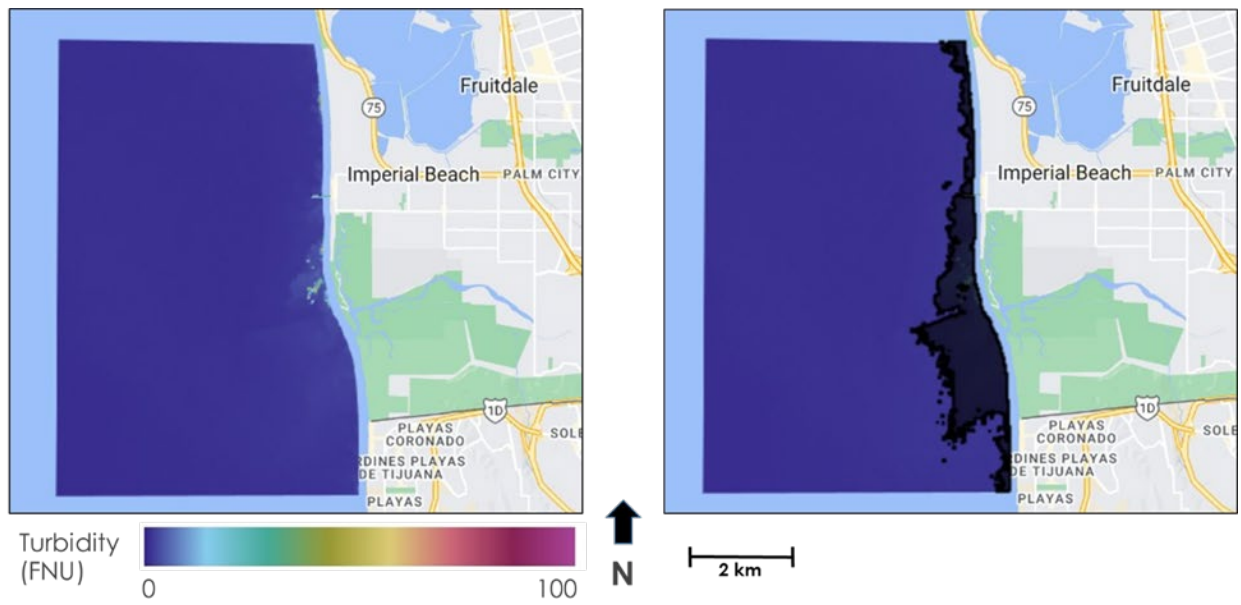


Figure C2. Mixed plume turbidity image from Sentinel-2 MSI on 3-6-2021 (left) and the plume delineation shapefile (right)